ORGANOMETALLICS

pubs.acs.org/Organometallics

Article

Synthesis and Characterization of New Counterion-Substituted Triacylgermenolates and Investigation of Selected Metal−Metal Exchange Reactions

Manfred Drusgala, Matthias Paris, Janine Maier, Roland C. Fischer, and Michael Haas*

Cite This: *Organometallics* 2022, 41, 2170−2179

Read Online

ACCESS | Metrics & More | Article Recommendations | Supporting Information

ABSTRACT: The synthetic process to obtain triacylgermenolates with alternated counterions by single-electron-transfer reactions or by a direct approach is described. The formation of these derivatives was confirmed by NMR spectroscopy and UV−vis spectroscopy. Moreover, metal−metal exchange reactions of potassium-substituted triacylgermenolate **2a** with $MgBr_2$, $ZnCl_2$, and $HgCl_2$ are presented. Additionally, **2a** was reacted with nBu$_4$NBr, which led to the formation of ammonia-substituted triacylgermenolate **8**. Furthermore, we reacted **2a** with HCl/Et$_2$O to obtain triacylgermane **9**. Subsequently, we investigated the reaction of **9** with tBu$_2$Zn and tBu$_2$Hg. NMR spectroscopy, single-crystal X-ray crystallography, and UV−vis spectroscopy are employed for analysis of structural properties.

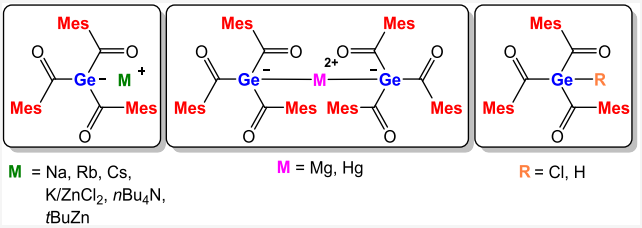

INTRODUCTION

Historically speaking, the synthesis and characterization of heavier group 14 (HG 14) enolates were mainly triggered by fundamental investigations in the field of main group chemistry.[1−5] Recently, we could demonstrate that HG 14 triacylenolates (M = Ge and Sn) represent innovative building blocks for the formation of high-performance free-radical photoinitiators.[6−8] To synthesize these new HG 14 triacylenolates, we established two pathways. The first methodology uses a potassium-induced single-electron-transfer (SET) approach starting from the respective tetraacyl derivatives. The second method uses the tetrakis(trimethylsilyl) derivatives as starting materials (direct approach). After KOtBu-induced desilylation and a reaction with 3 equiv of an acid fluoride, the respective HG 14 triacylenolates are obtained. The direct approach circumvents the usage of alkali metals and results in higher yields of the target compounds (Scheme 1). In general, the synthesis of HG 14 enolates was focused exclusively on lithium and potassium derivatives.[1−4,9−15] Other counterions were not investigated so far, although they can significantly influence the reactivity and the structural properties of these enolates. Consequently, the aim of this study was to introduce new counterions. Therein, we focused on germanium as the central atom and used exclusively the 2,4,6-trimethylphenyl moiety as an aromatic group at the carbonyl group.

RESULTS AND DISCUSSION

Electron-Transfer Reactions of Other Alkali Metals (Method A). Recently, we have investigated the usage of elemental lithium to induce electron-transfer reactions with tetraacylstannanes. However, only uncharacterizable polymers were found.[16] The same holds true for tetraacylgermanes. At the beginning of the reaction, the reaction solution changed from yellow to orange, which indicates the formation of the target compound. However, on prolonged stirring (approx. 30 min), the color changed to deep black, along with the formation of a precipitate. We assume that the initially formed lithium-substituted germenolate is highly unstable, and therefore, an isolation of the lithium derivative is not possible. On the basis of this observation, we investigated sodium as a reducing agent. Consequently, we reacted **1a** with 2.1 equiv of sodium in tetrahydrofuran (THF). The reaction solution was stirred overnight, and the complete consumption of the metal marks the end of the reaction. This germenolate **3a** is formed with remarkable selectivity, based on performed NMR spectroscopy at the end of the reaction. **3a** was isolated as a red solid in 74% yield by adding n-pentane to the reaction solution (see Scheme 2). Analytic and spectroscopic data that support the structural assignment together with experimental details are summarized in the Experimental Section.

We further investigated the usage of other alkali metals (rubidium, cesium) to synthesize differently decorated triacylgermenolates. In both cases, compound **1a** was reacted with 2.1 equiv of the respective metal in THF as solvent (Scheme 3). However, the high solubility of these heavier alkali

Received: May 25, 2022
Published: July 13, 2022

https://doi.org/10.1021/acs.organomet.2c00256
Organometallics 2022, 41, 2170−2179

Scheme 1. SET Approach vs Direct Approach

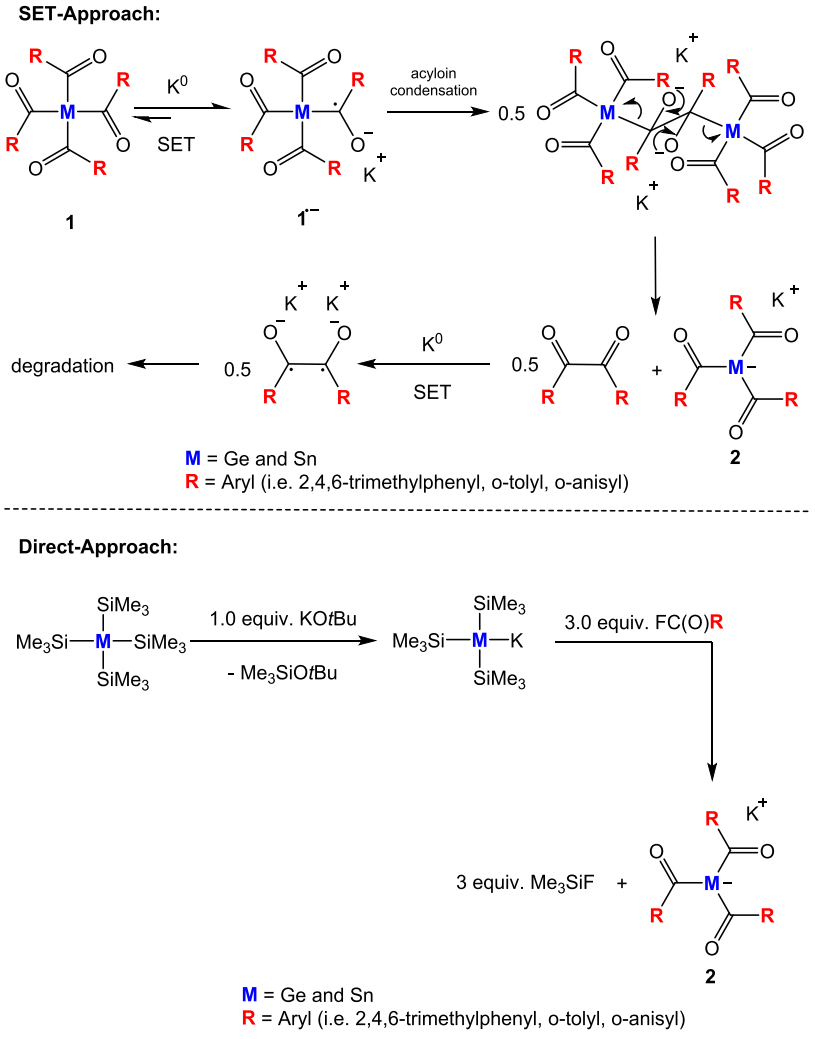

Scheme 2. SET Reaction of 1a with Na^0

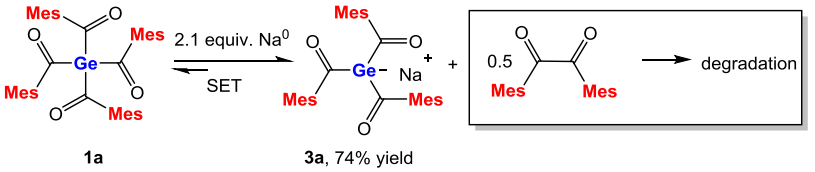

Scheme 3. SET Reaction of 1a with Rb^0 and Cs^0

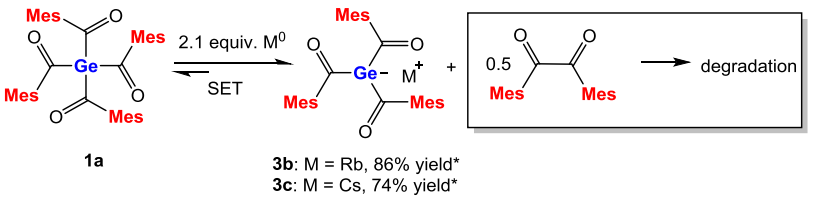

metals prevented the isolation of these compounds via the SET approach. Experimental details are summarized in the Experimental Section, and NMR spectra of the reaction solutions are provided in the Supporting Information.

Direct Approach toward Triacylgermenolates (Method B). As outlined in the Introduction section, the direct approach is a convenient method to obtain potassium triacylgermenolates, with various substituents on the carbonyl group in good to excellent yields. Here, we used other metal-*tert*-butoxides (NaO*t*Bu, RbO*t*Bu, and CsO*t*Bu) to generate the germanide metal in situ.[17,18] These germanides were subsequently reacted with 3 equiv of mesitoylfluoride. The

https://doi.org/10.1021/acs.organomet.2c00256
Organometallics 2022, 41, 2170−2179

Scheme 4. Direct Approach toward 4a−c

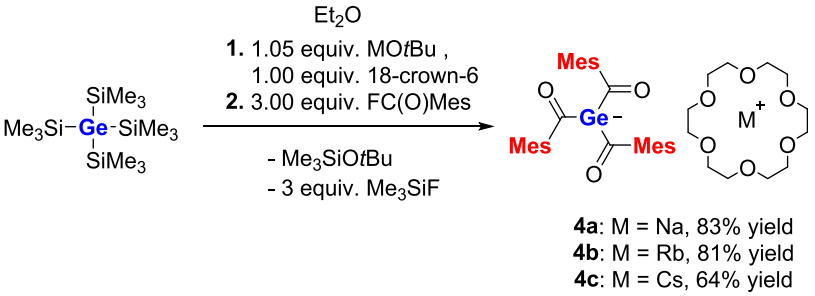

addition of 18-crown-6 is necessary to induce precipitation of the formed germenolates in Et_2O (see Scheme 4). Compounds **4a−c** were isolated in good to excellent yields (experimental details are included in the Experimental Section).

Stability of 3a and 4a−c. All isolated germenolates can be stored in the absence of air at room temperature for prolonged time (usually months).

UV−vis spectroscopy of 2a, 3a, and 4a−c. To determine the longest absorption band for our isolated germenolates, we used THF as the solvent and compared it with the parent compound **2a** (M = K). In Figure 1, the

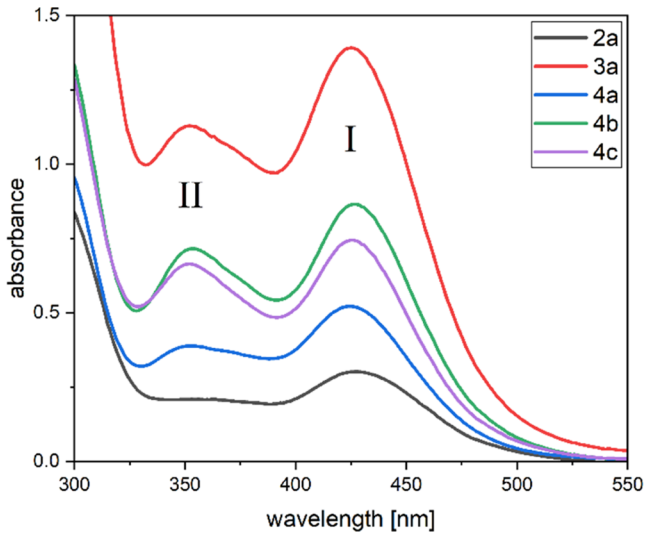

Figure 1. Measured UV−vis spectra of **2a**, **3a**, and **4a−c** in THF (1×10^{-4} mol/L).

measured UV−vis spectra of the isolated germenolates are depicted. These germenolates exhibit two distinct absorption bands with λ_{max} = 425−427 nm (band I [pz-π* excitation]) and 352−353 nm (band II [π-π* excitation]).

Transmetalation Reactions of 2a. In contrast to metal enolates where magnesium as a counterion is widely used,[19,20] an HG 14 magnesium-substituted enolate has not been reported so far. Therefore, we reacted our potassium triacylgermenolate **2a** with 0.55 equiv of $MgBr_2$ in THF at −30 °C. After removal of the solvent and resuspension in toluene, the reaction salt was filtered off the reaction solution. Compound **5** was isolated by crystallization in excellent yield (Scheme 5).

Furthermore, we were able to structurally confirm compound **5** by single-crystal X-ray diffraction analysis (compare Figure 2). **5** crystallizes in monoclinic space group

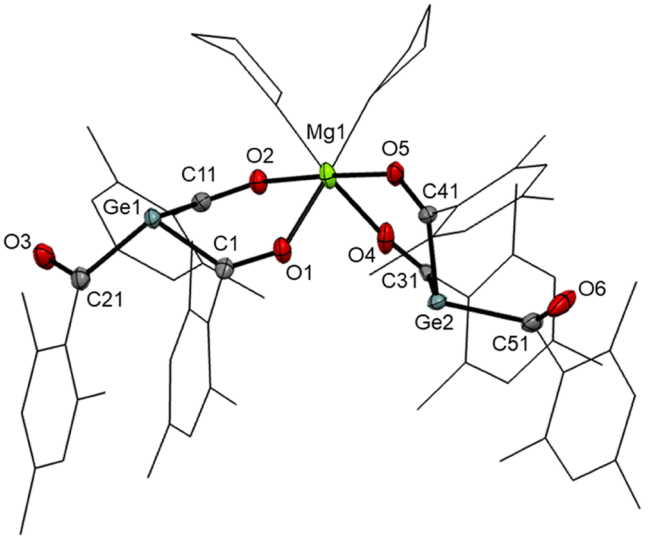

Figure 2. ORTEP representation for compound **5**. Thermal ellipsoids are depicted at the 50% probability level. Hydrogen atoms are omitted, and mesityl groups and THF molecules are displayed as wireframes for clarity. Selected bond lengths (Å) and bond angles (deg) with estimated standard deviations: ∑αGe(1) 308.38, ∑αGe(2) 308.11, Ge(1)−C(1) 2.004 (3), Ge(1)−C(11) 2.006 (3), Ge(1)−C(21) 2.029 (3), C(1)−O(1) 1.252 (3), C(11)−O(2) 1.250 (3), C(21)−O(3) 1.223 (4), Mg(1)−O(1) 2.060 (2), Mg(1)−O(2) 2.043 (2), Mg(1)−O(4) 2.055 (2), Mg(1)−O(5) 2.047 (2), Mg(1)−O(THF) 2.093, C(31)−O(4) 1.167 (9), C(41)−O(5) 1.192 (6), C(51)−O(6) 1.220 (7), Ge(2)−C(31) 2.007 (8), Ge(2)−C(41) 1.988 (5), Ge(2)−C(51) 2.036 (6).

Scheme 5. Reaction of 2a with $MgBr_2$

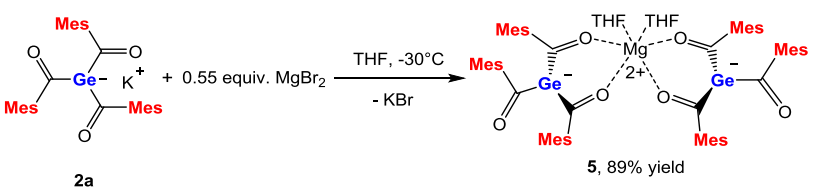

https://doi.org/10.1021/acs.organomet.2c00256
Organometallics 2022, 41, 2170−2179

Scheme 6. Reaction of 2a with $ZnCl_2$

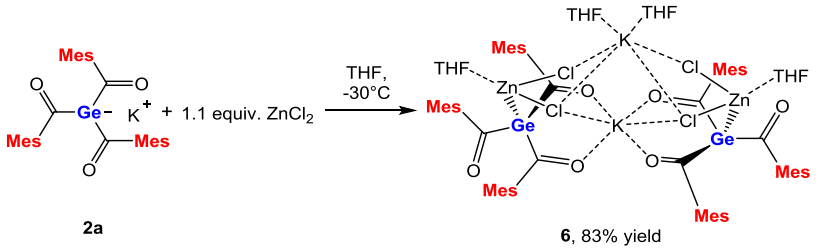

$P2\bar{1}n$ and the unit cell contains four molecules. In close analogy to other structurally characterized germenolates,[6−9,12,13] the central Ge atoms are pyramidal and have elongated Ge−C single bonds. Noteworthy is an interesting structural feature in the structure of **5**. The relative orientation of the six carbonyl groups is different. While four groups are orientated to the magnesium center, the remaining other two groups do not show any coordination. This coordination is also found in solution, as all signals for the mesityl groups in the ^{1}H and ^{13}C NMR spectra are in the 2:1 ratio (the solvent for NMR spectra is THF-d_8). Furthermore, two additional donor molecules of THF coordinate to the magnesium atom (experimental details are included in Experimental Section).

The next synthetic target was the synthesis of an HG 14 zinc enolate. Therefore, we reacted **2a** with 0.55 equiv of $ZnCl_2$. However, NMR spectroscopy performed after the addition of the zinc salt showed the formation of a new product along with the remaining starting material in the ratio of 1:1. Consequently, we added another 0.55 equiv of $ZnCl_2$ to the reaction solution and observed the complete consumption of the starting material and the formation of one single product. After removal of the solvent, resuspension in toluene, and filtration, compound **6** was isolated in 83% yield (see Scheme 6). In contrast to the magnesium enolate, compound **6** shows only one signal for the three carbonyl groups and four for the aryl carbon atoms in the ^{13}C NMR spectrum. This indicates a better solvent separation for this compound. NMR spectra and detailed assignments are provided in Experimental Section and in the Supporting Information.

Single crystals suitable for X-ray analysis were obtained by cooling the concentrated solution of **6** in THF to −30 °C (Figure 3). Compound **6** crystallized in the monoclinic space group $C\bar{2}c$, and the unit cell contains four molecules. Again, the central germanium atoms are pyramidal and the Ge−C bonds are elongated. The structural analysis also sheds light on the experimental observations that no salt was formed. In contrast to the expected transmetalation, the first bimetallic HG 14 enolate is formed. This so-called zincate forms a dimer bridged by two potassium atoms, which have two different coordination modes. K(1) is coordinatively saturated by two chlorine atoms and four oxygen atoms. K(2) is coordinated by two THF molecules and four chlorine atoms. Moreover, the Zn−Ge bond length of 2.448 Å is slightly longer than their covalent radii (2.42 Å) and significantly longer than those of $[Ph_3Ge]_2Zn$,[21] $(Me_3Si)_3GeZnCl$,[22] and $[(Me_3Si)_3Ge]_2Zn$.[23]

Reaction of 2a with $HgCl_2$. On the basis of the observed reactivity with $ZnCl_2$, we wanted to investigate the outcome of the reaction of **2a** with mercury dichloride. Therefore, we reacted **2a** with equimolar amounts of $HgCl_2$ at −70 °C in THF (see Scheme 7). After removal of the solvent and the formed salts, the reaction control by NMR spectroscopy showed the formation of a sole germanium-based product with

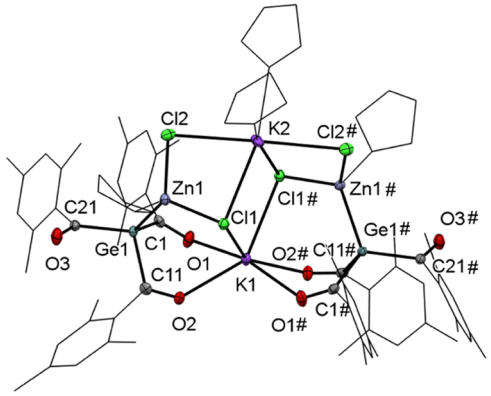

Figure 3. ORTEP representation for compound **6**. Thermal ellipsoids are depicted at the 50% probability level. Hydrogen atoms are omitted, and mesityl groups and THF molecules are displayed as wireframes for clarity. Selected bond lengths (Å) and bond angles (deg) with estimated standard deviations: $\sum\alpha$Ge(1) 317.91, Ge(1)−C(1) 2.050 (3), Ge(1)−C(11) 2.046 (3), Ge(1)−C(21) 2.048 (3), C(1)−O(1) 1.224 (4), C(11)−O(2) 1.217 (4), C(21)−O(3) 1.221 (4), K(1)−O(1) 2.651 (2), K(1)−O(2) 2.742 (2), Zn(1)−Ge(1) 2.4475 (5), Zn(1)−Cl(1) 2.2793 (9), Zn(1)−Cl(2) (2.2688 9), K(1)−Cl(1) 3.1512 (11), K(2)−Cl(1) 3.1350 (11), K(2)−Cl(2) 3.1236 (9).

a characteristic shift for an acylgermane (^{13}C NMR shifts for the carbonyl group δ = 227.86 ppm). We consequently assumed that the expected Ge−Hg−Cl bond was formed. However, structural analysis revealed our preliminary assumption to be wrong. Instead of the expected product, chlorotrimesitoylgermane **7** was formed in good yields (see Figure 4). Here, we assume that the initial compound is thermally unstable and eliminates elemental mercury. Satgé and coworkers found a similar reactivity for their germanium−mercury derivative.[24]

Compound **7** crystallized in the monoclinic space group $P21$ and the unit cell contains 14 molecules. Additionally, this compound represents an interesting new building block as it can be used as the precursor for further derivatization.

Reaction of 2a with Tetrabutylammonium Bromide. In several conferences, we were asked about the reactivity of our germenolates with ammonium salts. As solubility is always an issue for this type of compounds, we thought that the ammonium counterions can contribute to solving this problem. Consequently, we set out and reacted **2a** with equimolar amounts of nBu$_4$NBr in toluene at 0 °C. After removal of the salts, compound **8** was isolated in 83% yield as a red oil (see Scheme 8). NMR spectra and detailed assignments are provided in Experimental Section and in the Supporting Information. As expected, compound **8** has good solubility in polar as well as nonpolar solvents. Moreover, compound **8** is

https://doi.org/10.1021/acs.organomet.2c00256
Organometallics 2022, 41, 2170−2179

Scheme 7. Reaction of 2a with $HgCl_2$

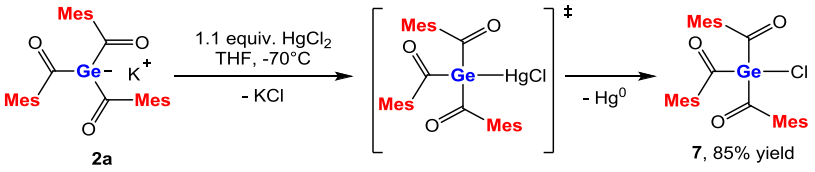

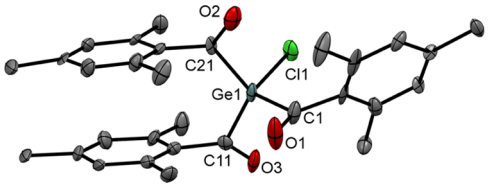

Figure 4. ORTEP representation for compound **7**. Thermal ellipsoids are depicted at the 50% probability level. Hydrogen atoms are omitted for clarity. Selected bond lengths (Å) with estimated standard deviations: Ge(1)−Cl(1) 2.173(3), Ge(1)−C(1) 2.018(11), Ge(1)−C(11) 2.070 (11), Ge(1)−C(21) 2.023(11), C(1)−O(1) 1.215(15), C(11)−O(3) 1.201(14), C(21)−O(2) 1.175(14).

highly stable, as no degradation was observed even at room temperature.

Reaction of 2a with HCl. Given the well-known reactivity of germanides with protic solvents to form germanes,[25,26] we investigated the reaction of **2a** with MeOH, EtOH, and H_2O. With these above-mentioned reagents, we observed the formation of the expected product; however, we also found the formation of multiple uncharacterized side products. Therefore, we set out and tested the reaction with HCl dissolved in Et_2O. To our delight, we found more selective reactivity and compound **9** was isolated in excellent yields (see Scheme 9). NMR spectra and detailed assignments are provided in Experimental Section and in the Supporting Information. A characteristic of compound **9** is the significant low-field-shifted ^{1}H NMR signal for the hydrogen bonded to the germanium atom with δ = 6.29 ppm.

The so-obtained compound **9** is also an interesting precursor molecule, as the labile Ge−H bond can be used for the formation of selected examples of oligoacyldigermanes. Therefore, we reacted **9** with an organozinc and an organomercury reagent.

Reaction of 9 with tBu$_2$Zn. Following the seminal work of Apeloig and co-workers who presented the first examples of radical activation of the Si−H bond with organozinc reagents,[27] we reacted **9** with 0.5 equiv of tBu$_2$Zn. After the addition of the organozinc reagent, an orange precipitate was immediately formed, which was filtered off. However, in the reaction solution, we found significant amounts of unreacted starting material, and moreover, tBu$_2$Zn was completely consumed. Therefore, we attempted to characterize the orange precipitate and found that the compound decomposes immediately in polar solvents (i.e., THF, Et_2O) to a complex product mixture with no traces of the desired product. In nonpolar solvents, the compound has very low solubility, which prevented complete characterization. However, the ^{1}H NMR spectrum indicated that compound **9** reacts with tBu$_2$Zn to form an unexpected product. Unfortunately, it was not possible to obtain a ^{13}C NMR spectrum of sufficient quality due to low solubility. First, we assumed that this product is an intermediate as a significant amount of starting material was still found in the reaction solution. Consequently, we prolonged the stirring at room temperature (48 h) and changed the reaction conditions (90 °C for 24 h), but no other product was found. The structural determination shed light on the structure of this compound. In Figure 5, the structure of compound **10** is depicted. As assumed, the triacylgermane reacts with tBu$_2$Zn, but after the first radical reaction, the zinc atom is coordinatively saturated by two oxygen atoms and this prevented a further reaction of this compound. Moreover, based on the sterical hindrance, we found three signals for the mesityl protons in the ^{1}H NMR spectrum.

Compound **10** crystallized in the triclinic space group $\bar{P}1$, and the unit cell contains two molecules. The central germanium atoms are again pyramidal, and the Ge−C bonds are significantly elongated. Moreover, the Zn−Ge bond length is significantly elongated in comparison to their covalent radii and comparable examples.[21−23] On the basis of the structural analysis, we re-evaluated our reaction and reacted **9** with equimolar amounts of tBu$_2$Zn to determine the selectivity of this reaction. To our delight, we found that the reaction is very selective and compound **10** was isolable nearly quantitatively (see Scheme 10).

Reaction of 9 with tBu$_2$Hg. With tBu$_2$Hg, the metalation of the Ge−H bond was much smoother. Compound **9** was reacted in n-heptane with tBu$_2$Hg and stirred at 70 °C for 18 h. The corresponding digermylmercury compound **11** was obtained in 81% yield (see Scheme 11). NMR spectra and detailed assignments are provided in Experimental Section and in the Supporting Information.

NMR Spectroscopy. The observed ^{13}C NMR shifts of the carbonyl C atoms of all isolated germenolates **2a**, **3a−c**, **4a−c**,

Scheme 8. Reaction of 2a with nBu$_4$NBr

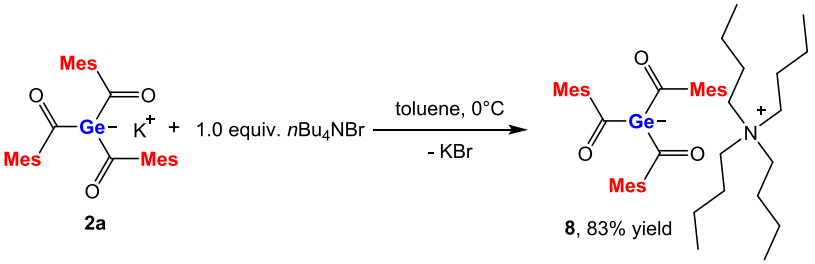

https://doi.org/10.1021/acs.organomet.2c00256
Organometallics 2022, 41, 2170−2179

Scheme 9. Reaction of 2a with HCl/Et_2O

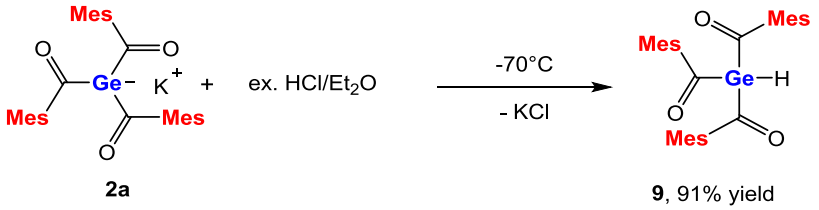

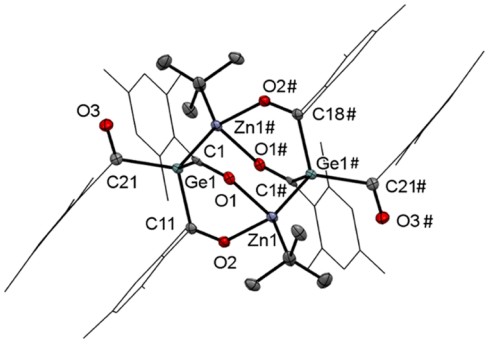

Figure 5. ORTEP representation for compound **10**. Thermal ellipsoids are depicted at the 50% probability level. Hydrogen atoms are omitted, and the mesityl groups are displayed as wireframes for clarity. Selected bond lengths (Å) and bond angles (deg) with estimated standard deviations: $\sum\alpha$Ge(1) 313.89, Ge(1)−C(1) 2.019 (3), Ge(1)−C(11) 2.026 (18), Ge(1)−C(21) 2.050 (19), C(1)−O(1) 1.242 (2), C(11)−O(2) 1.244 (2), C(21)−O(3) 1.215 (2), Zn(1)−O(1) 2.1211 (13), Zn(1)−O(2) 2.1181 (13), Zn(1)−Ge(1) 2.4902 (3).

5, **6**, and **8** were found in the region between δ = 247.83 and 274.88 ppm, which is typical for carbonyl groups attached to the negatively charged germanium atoms. In contrast to this, all carbonyl C atoms of acylgermanes **7**, **9**, and **11** were found significantly high field shifted between δ = 227.86 and 238.17. Again, this correlates well with all carbonyl C shifts of other known acylgermanes (see Table 1).[6,7,28,29]

CONCLUSIONS

In summary, we investigated the synthesis of a variety of new triacylgermenolates by a single-electron-transfer reaction or by a direct approach. The single-electron-transfer reactions were induced by the respective alkali metals (sodium, rubidium, or cesium). In all cases, the formation of triacylgermenolates (**3a−c**) was observed. However, the high solubility of the rubidium and cesium derivatives prevented the complete isolation. For the direct approach, the respective tris(trimethylsilyl)germanides were synthesized by base-mediated desilylation of tetrakis(trimethylsilyl)germane with metal-*tert*-butoxides (NaO*t*Bu, RbO*t*Bu, and CsO*t*Bu) and reacted with 3 equiv of mesitoylfluoride. The addition of 18-crown-6 was necessary to induce precipitation of the formed germenolate in Et_2O. Compounds **4a−c** were isolated in good to excellent yields and completely characterized. Furthermore, we performed selected transmetalation of potassium-substituted germenolate **2a** with $MgBr_2$, $ZnCl_2$, and $HgCl_2$. In the case of the magnesium salt, we found the formation of the expected magnesium-bridged derivative **5** in excellent yield, which represents the first magnesium-coordinated HG 14 enolate. $ZnCl_2$ reacts with **2a** under the formation of the first bimetallic HG 14 enolate **6**. The attempted transmetalation with $HgCl_2$ did not lead to the expected product. Instead, the formation of chloro-trimesitoylgermane **7** was observed. Furthermore, we reacted **2a** with *n*Bu_4NBr and found selective formation to the corresponding ammonium germenolate **8**. The reaction of **2a** with HCl/Et_2O led to the formation of the corresponding acylgermane **9**. Compound **9** was reacted with *t*Bu_2Zn and *t*Bu_2Hg to synthesize oligoacyldigermanes. While the reaction of **9** with *t*Bu_2Hg yields the expected digermylmercury compound **11**, the reaction with *t*Bu_2Zn stopped after the first radical reaction and compound **10** is formed quantitatively. Further studies to investigate the reactivity of these new germenolates are currently in progress. In addition, we are currently testing compound **7** as a new building block for further derivatization.

EXPERIMENTAL SECTION

General Procedures. All experiments were performed under a nitrogen atmosphere using standard Schlenk techniques. Solvents were dried using a column solvent purification system.[30] Me_3SiCl (≥99%), $GeCl_4$ (>99.99%), KO*t*Bu (>98%), NaO*t*Bu (97%), ClC(O)Mes (98%), 18-crown-6 (99%), potassium (98%), sodium (98%), rubidium (99.6%), cesium (≥99.95%), HCl gas (3.0; 99,9%), THF-d_8 (99.5 atom% D), C_6D_6 (99.5 atom%, D), and $CDCl_3$ (99.8 atom% D) were used without any further purification. Salts were dried before usage. For the measurement of air-sensitive samples, deuterated solvents were additionally dried (C_6D_6 was dried by 24 h reflux above a sodium/potassium alloy; THF-d_8 was dried by 6 h reflux above lithium aluminum hydride). Cesium-*tert*-butoxide,[31] rubidium-*tert*-butoxide,[31] di-*tert*-butylmercury[32] (note: as organomercury compounds are acutely toxic by all exposure routes, all operations involving this compound should be carried out in a certified chemical fume hood or glovebox), di-*tert*-butylzinc,[33] tetrakis(2,4,6-trimethylbenzoyl)germane,[34] and potassium-tris(2,4,6-

Scheme 10. Reaction of 9 with *t*Bu_2Zn

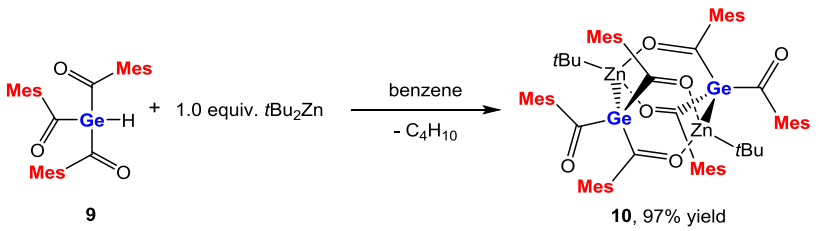

https://doi.org/10.1021/acs.organomet.2c00256
Organometallics 2022, 41, 2170−2179

Scheme 11. Reaction of 9 with tBu$_2$Hg

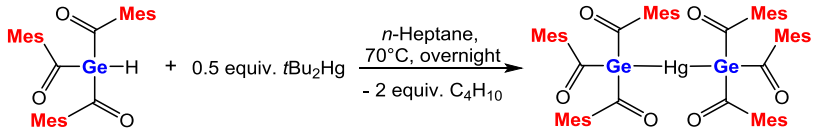

9 **11**, 81% yield

Table 1. ^{13}C NMR Shifts of the Carbonyl Atoms for Compounds 3a−c, 4a−c, 5−9, and 11

com	^{13}C NMR (ppm)	com	^{13}C NMR (ppm)	com	^{13}C NMR (ppm)
2a	263.14[a]	**4b**	261.15[b]	**8**	261.45[b]
3a	263.75[a]	**4c**	260.99[b]	**9**	231.20[b]
3b	262.13[a]	**5**	247.83[a]	**11**	238.17[b]
			274.88[a]		
3c	261.66[a]	**6**	248.75[a]		
4a	262.68[b]	**7**	227.86[b]		

[a]Measured in THF-d_8 at RT. [b]Measured in C_6D_6 with 18-crown-6 at RT.

trimethylbenzoyl)germanide•0.5 DME[6] were prepared according to the published procedures. ^{1}H and ^{13}C NMR spectra were recorded either on a Varian INOVA 300 MHz, a Bruker AVANCE DPX 200 MHz, or a Bruker Avance 300 MHz spectrometer in C_6D_6 or THF-d_8 solution or with D_2O capillary and referenced vs TMS using the internal 2H-lock signal of the solvent. Infrared spectra were obtained on a Bruker α-P Diamond ATR Spectrometer from the solid sample. Melting points were determined using a Stuart SMP50 apparatus and were uncorrected. Elemental analyses were carried out on a Hanau Vario Elementar EL apparatus. UV−vis absorption spectra were recorded on a PerkinElmer Lambda 5 spectrometer.

X-ray Crystallography. All crystals suitable for single-crystal X-ray diffractometry were removed from a vial or Schlenk flask and immediately covered with a layer of silicone oil. A single crystal was selected, mounted on a glass rod on a copper pin, and placed in a cold N_2 stream. XRD data collection for compounds **5**, **6**, **7**, and **10** was performed on a Bruker APEX II diffractometer with the use of an Incoatec microfocus sealed tube of Mo Kα radiation (λ = 0.71073 Å) and a CCD area detector. Empirical absorption corrections were applied using SADABS or TWINABS.[35,36] The structures were solved with either the use of direct methods or the intrinsic phasing option in SHELXT and refined by the full-matrix least-squares procedures in SHELXL[37−39] or Olex2.[40] The space group assignments and structural solutions were evaluated using PLATON.[41,42] Non-hydrogen atoms were refined anisotropically. Hydrogen atoms were either located in a difference map or in calculated positions corresponding to the standard bond lengths and angles. The disorder was handled by modeling the occupancies of the individual orientations using free variables to refine the respective occupancy of the affected fragments (PART).[43] Table S1 in the Supporting Information contains crystallographic data and details of measurements and refinement for all compounds. Crystallographic data (excluding structure factors) have been deposited with the Cambridge Crystallographic Data Centre (CCDC) under the following numbers (**5**, 2174956; **6**, 2174957; **7**, 2174958; **10**, 2174959)

Synthesis of ***3a***. To a solution of 500 mg of tetrakis(2,4,6-trimethylbenzoyl)germane (0.76 mmol; 1.00 equiv) in 10 mL of THF, 37 mg of sodium (1.59 mmol; 2.10 equiv) was added at −70 °C. The reaction mixture was brought to room temperature and stirred overnight, turning into a red solution. The next day, the product was precipitated out of solution using n-pentane. It was filtrated off, subsequently, giving the product as a red solid. Yield: 300 mg (0.56 mmol; 74%) of analytically pure **3a** as a red crystalline solid. Mp: decomposition > 200 °C. Anal. calcd (%) for $C_{30}H_{33}GeNaO_3$: C, 67.07; H, 6.19, found: C, 67.23; H, 6.21. ^{13}C NMR data (THF-d_8, TMS, ppm): 263.75 (*C*═O), 148.43 (Mes-*C4*), 135.52 (Mes-*C1*), 131.75 (Mes-*C2*), 128.63 (Mes-*C3*), 21.42, 20.46 (Aryl-CH_3). ^{1}H NMR data (THF-d_8, TMS, ppm): 6.36 (s, 6H, Mes-*H*), 2.11 (s, 9H, Mes-CH_3), 2.00 (s, 18H, Mes-CH_3). UV−vis: λ [nm] (ε [L/mol/cm]) = 425 (13 900), 352 (11 290). IR (neat): ν(C═O) = 1640, 1605.

Synthesis of ***3b***. To a solution of 100 mg of tetrakis(2,4,6-trimethylbenzoyl)germane (0.15 mmol; 1.00 equiv) in 5 mL of THF, 27 mg of rubidium (0.32 mmol; 2.10 equiv) was added. The reaction mixture was stirred overnight, turning into a red solution. Due to the good solubility of the product, isolation was not possible. Conversion of the starting material was monitored by NMR spectroscopy with D_2O capillary of the crude reaction solution. Yield: 78 mg (0.13 mmol; 86%) of **3b** estimated by NMR spectroscopy. ^{13}C NMR data (D_2O, TMS, ppm): 262.13 (*C*═O), 147.92 (Mes-*C4*), 134.60 (Mes-*C1*), 131.00 (Mes-*C2*), 127.82 (Mes-*C3*), 20.62, 19.65 (Aryl-CH_3). ^{1}H NMR data (D_2O, TMS, ppm): 6.36 (s, 6H, Mes-*H*), 2.12 (s, 9H, Mes-CH_3), 1.99 (s, 18H, Mes-CH_3).

Synthesis of ***3c***. To a solution of 100 mg of tetrakis(2,4,6-trimethylbenzoyl)germane (0.15 mmol; 1.00 equiv) in 5 mL of THF, 42 mg of cesium (0.32 mmol; 2.10 equiv) was added. The reaction mixture was stirred overnight, turning into a red solution. Due to the good solubility of the product, isolation was not possible. Conversion of the starting material was monitored by NMR spectroscopy with D_2O capillary of the crude reaction solution. Yield: 72 mg (0.11 mmol; 74%) of **3c** estimated by NMR spectroscopy. ^{13}C NMR data (D_2O, TMS, ppm): 261.66 (*C*═O), 147.91 (Mes-*C4*), 134.68 (Mes-*C1*), 131.09 (Mes-*C2*), 127.88 (Mes-*C3*), 20.62, 19.65 (Aryl-CH_3). ^{1}H NMR data (D_2O, TMS, ppm): 6.36 (s, 6H, Mes-*H*), 2.11 (s, 9H, Mes-CH_3), 1.99 (s, 18H, Mes-CH_3).

Synthesis of ***4a***. In total, 1.00 g of tetrakis(trimethylsilyl)germane (2.74 mmol; 1.00 equiv) and 723 mg of 18-crown-6 (2.74 mmol; 1.00 equiv) were dissolved in 25 mL of Et_2O; then, 276 mg of NaOtBu (2.87 mmol; 1.05 equiv) was added. The solution was stirred at room temperature for 1 h. After full conversion (monitored by NMR spectroscopy), 456 mg of 2,4,6-trimethylbenzoyl fluoride (2.74 mmol, 1.00 equiv) was added and then stirred for 15 min. The second and the third equivalent were added in small portions after another 15 and 30 min, respectively. The reaction is stirred for another 2 h. The orange crystalline product was filtered off, washed with cold Et_2O, and dried in vacuum. Yield: 1.83 g (2.28 mmol; 83%) of analytically pure **4a** as an orange crystalline solid. Mp: 110−115 °C. Anal. calcd (%) for $C_{42}H_{57}GeNaO_9$: C, 62.94; H, 7.17, found: C, 62.70; H, 7.14. ^{13}C NMR data (C_6D_6, TMS, ppm): 262.68 (*C*═O), 148.24 (Mes-*C4*), 135.13 (Mes-*C1*), 131.39 (Mes-*C2*), 128.45 (Mes-*C3*), 69.72 ((-CH_2-CH_2-O-)$_6$), 21.27, 20.41 (Aryl-CH_3). ^{1}H NMR data (C_6D_6, TMS, ppm): 6.60 (s, 6H, Mes-*H*), 3.29 (s, 24H, (−CH_2−CH_2−O−)$_6$), 2.47 (s, 18H, Mes-CH_3), 2.18 (s, 9H, Mes-CH_3). UV−vis: λ [nm] (ε [L/mol/ cm]) = 425 (5212), 352 (3884). IR (neat): ν(C═O) = 1640, 1605.

Synthesis of ***4b***. In total, 1.00 g of tetrakis(trimethylsilyl)germane (2.74 mmol; 1.00 equiv) and 723 mg of 18-crown-6 (2.74 mmol; 1.00 equiv) were dissolved in 25 mL of Et_2O; then, 456 mg of RbOtBu (2.87 mmol; 1.05 equiv) was added. The solution was stirred at room temperature for 1 h. After full conversion (monitored by NMR spectroscopy), 456 mg of 2,4,6-trimethylbenzoyl fluoride (2.74 mmol, 1.00 equiv) was added and then stirred for 15 min. The second and the third equivalent were added in small portions after another 15 and 30 min, respectively. The reaction is stirred for another 2 h. The orange crystalline product was filtered off, washed with cold DME, and dried in vacuum. Yield: 1.91 g (2.21 mmol; 81%) of analytically

https://doi.org/10.1021/acs.organomet.2c00256
Organometallics 2022, 41, 2170−2179

pure **4b** as an orange crystalline solid. Mp: 71−76 °C. Anal. calcd (%) for $C_{42}H_{57}GeRbO_9$: C, 58.39; H, 6.65, found: C, 58.61; H, 6.62. ^{13}C NMR data (C_6D_6, TMS, ppm): 261.15 (*C*=O), 148.49 (Mes-*C*4), 134.98 (Mes-*C*1), 131.53 (Mes-*C*2), (Mes-*C*3 superimposed by C_6D_6 signals), 70.22 ((−CH_2−CH_2−O−)$_6$), 21.28, 20.43 (Aryl-CH_3). ^1H NMR data (C_6D_6, TMS, ppm): 6.61 (s, 6H, Mes-*H*), 3.20 (s, 24H, (−CH_2−CH_2−O−)$_6$), 2.50 (s, 18H, Mes-CH_3), 2.19 (s, 9H, Mes-CH_3). UV−vis: λ [nm] (ε [L/mol/cm]) = 427 (8647), 353 (7153). IR (neat): ν(C=O) = 1642, 1606.

Synthesis of ***4c***. In total, 800 mg of tetrakis(trimethylsilyl)germane (2.19 mmol; 1.00 equiv) and 579 mg of 18-crown-6 (2.19 mmol; 1.00 equiv) were dissolved in 25 mL of Et_2O; then, 474 mg of CsO*t*Bu (2.30 mmol; 1.05 equiv) was added. The solution was stirred at room temperature for 1 h. After full conversion (monitored by NMR spectroscopy), 364 mg of 2,4,6-trimethylbenzoyl fluoride (2.19 mmol, 1.00 equiv) was added and then stirred for 15 min. The second and the third equivalent were added in small portions after another 15 and 30 min, respectively. The reaction was stirred for another 2 h. The orange crystalline product was filtered off, washed with cold Et_2O, and dried in vacuum. Yield: 1.27 g (1.39 mmol; 64%) of analytically pure **4c** as an orange crystalline solid. Mp: 72−77 °C. Anal. calcd (%) for $C_{42}H_{57}GeCsO_9$: C, 55.35; H, 6.30, found: C, 55.21; H, 6.28. ^{13}C NMR data (C_6D_6, TMS, ppm): 260.99 (*C*=O), 148.50 (Mes-*C*4), 134.92 (Mes-*C*1), 131.55 (Mes-*C*2), (Mes-*C*3 superimposed by C_6D_6 signals), 70.11 ((−CH_2−CH_2−O−)$_6$), 21.30, 20.48 (Aryl-CH_3). ^1H NMR data (C_6D_6, TMS, ppm): 6.60 (s, 6H, Mes-*H*), 3.10 (s, 24H, (−CH_2−CH_2−O−)$_6$), 2.51 (s, 18H, Mes-CH_3), 2.18 (s, 9H, Mes-CH_3). UV−vis: λ [nm] (ε [L/mol/cm]) = 425 (7434), 352 (6640). IR (neat): ν(C=O) = 1639, 1607.

Synthesis of ***5***. To a solution of 400 mg of potassium-tris(2,4,6-trimethylbenzoyl)germanide·0.5 DME (0.67 mmol; 1.00 equiv) in 10 mL of THF, 68 mg of magnesium bromide (0.37 mmol; 0.55 equiv) in 10 mL of THF was added at −30 °C via a syringe. The reaction mixture was brought to room temperature, and the solvent was removed. The crude product was resolved in toluene and filtered via a syringe filter. Then, the toluene was partly removed and the product was recrystallized and isolated. Yield: 313 mg (0.30 mmol, 89%) of analytically pure **5** as a red crystalline solid. Mp: 197−198 °C. Anal. calcd (%) for $C_{60}H_{66}Ge_2MgO_6$: C, 68.46; H, 6.32, found: C, 68.43; H, 6.63. ^{13}C NMR data (THF-d_8, TMS, ppm): 274.88, 247.83 (*C*=O), 146.28, 136.54, 131.82, 128.85. 146.34, 137.11, 132.32, 128.92 (Mes-*C*), 20.82, 21.41, 21.40, 20.13 (Aryl-CH_3). ^1H NMR data (THF-d_8, TMS, ppm): 6.52 (s, 8H, Mes-*H*), 6.28 (s, 4H, Mes-*H*), 2.19 (s, 12H, Mes-CH_3), 2.12 (s, 6H, Mes-CH_3), 2.08 (s, 24H, Mes-CH_3), 1.87 (s, 12H, Mes-CH_3). UV−vis: λ [nm] (ε [L/mol/cm]) = 435 (17394), 366 (8912). IR (neat): ν(C=O) = 1644, 1606.

Synthesis of ***6***. To a solution of 400 mg of potassium-tris(2,4,6-trimethylbenzoyl)germanide·0.5 DME (0.67 mmol; 1.00 equiv) in 10 mL of THF, 50 mg of zinc chloride (0.37 mmol; 0.55 equiv) in 10 mL of THF was added at −30 °C via a syringe. The reaction mixture was brought to room temperature, and the conversion was monitored by NMR spectroscopy. Since the starting material was only half-consumed, another 50 mg of zinc chloride (0.37 mmol; 0.55 equiv) in 10 mL of THF was added at −30 °C. After bringing the mixture to room temperature and checking for full consumption of the starting material via NMR spectroscopy, the solvent was removed. The crude product was resuspended in toluene and filtered via a syringe filter. Then, the toluene was removed and the product was isolated. Yield: 380 mg (0.28 mmol; 83%) of analytically pure **6** as a yellow crystalline solid. Mp: decomposition > 170 °C. Anal. calcd (%) for $C_{60}H_{66}Cl_4Ge_2K_2O_6Zn_2$: C, 52.25; H, 4.82, found: C, 52.52; H, 4.53. ^{13}C NMR Data (THF-d_8, TMS, ppm): 248.75 (*C*=O), 145.63 (Mes-*C*4), 137.92 (Mes-*C*1), 133.18 (Mes-*C*2), 129.01 (Mes-*C*3), 21.30, 20.47 (Aryl-CH_3). ^1H NMR Data (THF-d_8, TMS, ppm): 6.52 (s, 12H, Mes-*H*), 2.17 (s, 18H, Mes-CH_3), 2.04 (s, 36H, Mes-CH_3). UV−vis: λ [nm] (ε [L/mol/cm]) = 401 (2362), 382 (3017). IR (neat): ν(C=O) = 1640, 1609.

Synthesis of ***7***. To a solution of 500 mg of potassium-tris(2,4,6-trimethylbenzoyl)germanide·0.5 DME (0.83 mmol; 1.00 equiv) in 5 mL of THF, 216 mg of $HgCl_2$ (0.92 mmol; 1.1 equiv) was added at −70 °C. The reaction mixture was stirred for about an hour while warming up to room temperature. Subsequently, the solvent was removed in vacuum, and the product was resolved with toluene and filtrated using a syringe filter. Again, the solvent was removed in vacuum and the product was recrystallized using *n*-pentane. After storing the product at −30 °C overnight, **7** was isolated as a yellow solid. Yield: 392 mg (0.71 mmol; 85%) of analytically pure **7** as a yellow crystalline solid. Mp: 115−120 °C. Anal. Calcd (%) for $C_{30}H_{33}ClGeO_3$: C, 65.55; H, 6.05, found: C, 65.52; H, 6.05. ^{13}C NMR data (C_6D_6, TMS, ppm): 227.86 (*C*=O), 140.29 (Mes-*C*4), 140.16 (Mes-*C*1), 133.73 (Mes-*C*2), 129.29 (Mes-*C*3), 21.08, 19.46 (Aryl-CH_3). ^1H NMR data (C_6D_6, TMS, ppm): 6.47 (s, 6H, Mes-*H*), 2.21 (s, 18H, Mes-CH_3), 1.96 (s, 9H, Mes-CH_3). UV−vis: λ [nm] (ε [L/mol/cm]) = 401 (4262), 380 (6056). **IR** (neat): ν(C=O) = 1653, 1646, 1607.

Synthesis of ***8***. To a solution of 1.00 g of potassium-tris(2,4,6-trimethylbenzoyl)germanide·0.5 DME (1.67 mmol; 1,00 equiv) in 10 mL of THF, 538 mg of tetrabutylammonium bromide (1.67 mmol; 1.00 equiv) in 10 mL of toluene was added at 0 °C. The mixture was stirred for 30 min at room temperature. Subsequently, the solvent was removed in vacuum, and the product was resuspended in toluene and filtrated using a syringe filter. Then, *n*-pentane was added, resulting in the settling of red oil at the bottom of the flask. The solvents were carefully removed with a syringe, and the remaining oil was dried in vacuum. Yield: 1.05 g (1.39 mmol; 83%) of analytically pure **8** as a red oil. Anal. calcd (%) for $C_{46}H_{69}GeNO_3$: C, 73.02; H, 9.19; N 1.85, found: C, 72.87; H, 9.17; N 1.85. ^{13}C NMR data (C_6D_6, TMS, ppm): 261.45 (*C*=O), 149.24 (Mes-*C*4), 134.43 (Mes-*C*1), 131.50 (Mes-*C*2), 128.26 (Mes-*C*3), 58.20 (N−CH_2−), 24.07 (−CH_2−CH_2−CH_2−) 21.30 (Aryl-CH_3), 20.53 (−CH_2−CH_2−CH_3), 19.97 (Aryl-CH_3), 13.92 (−CH_2−CH_3). ^1H NMR data (C_6D_6, TMS, ppm): 6.53 (s, 6H, Mes-*H*), 3.08−3.03 (m, 8H, N−CH_2−), 2.43 (s, 18H, Mes-CH_3), 2.16 (s, 9H, Mes-CH_3), 1.35−1.24 (m, 8H, −CH_2−CH_2−CH_2−), 1.21−1.12 (m, 8H, −CH_2−CH_2−CH_3), 0.81 (t, 12H, −CH_2−CH_3). UV−vis: λ [nm] (ε [L/mol/cm]) = 425 (4555), 353 (4569). IR (neat): ν(C=O) = 1648, 1599.

Synthesis of ***9***. In total, 500 mg of potassium-tris(2,4,6-trimethylbenzoyl)germanide·0.5 DME (0.83 mmol; 1.00 equiv) in 5 mL of THF was added to 5 mL of HCl dissolved in Et_2O (16.80 mmol; 20.14 equiv, 3.36 M) at −70 °C via a syringe. The reaction mixture was brought to room temperature, and the solvent was removed. The crude product was resolved in toluene and filtered using a syringe filter. After removal of the solvent, the yellow oil was again dissolved in *n*-pentane. The product was then recrystallized at −70 °C and isolated. Yield: 391 mg (0.76 mmol; 91%) of analytically pure **9** as a yellow crystalline solid. Mp: 61−62 °C. Anal. calcd (%) for $C_{30}H_{34}GeO_3$: C, 69.94; H, 6.65, found: C, 69.89; H, 6.62. ^{13}C NMR data (C_6D_6, TMS, ppm): 231.20 (C=O), 142.78 (Mes-*C*4), 139.61 (Mes-*C*1), 133.16 (Mes-*C*2), 129.34 (Mes-*C*3), 21.06, 19.33 (Aryl-CH_3). ^1H NMR data (C_6D_6, TMS, ppm): 6.48 (s, 6H, Mes-*H*), 6.29 (s, 1H, Ge-*H*), 2.17 (s, 18H, Mes-CH_3), 1.99 (s, 9H, Mes-CH_3). UV−vis: λ [nm] (ε [L mol^{-1} cm^{-1}]) = 403 (964), 381 (1262). IR (neat): ν(C=O) = 1643, 1606.

Synthesis of ***10***. To a solution of 300 mg of **9** (0.58 mmol; 1.00 equiv) in 5 mL of benzene, 104 mg of di-*tert*-butylzinc (0.58 mmol; 1.00 equiv), dissolved in 4 mL of benzene, was added. The reaction mixture was stirred for 2 h. The product was filtered off and washed with benzene. Yield: 360 mg (0.28 mmol; 97%) of analytically pure **10** as an orange crystalline solid. Mp: 235−236 °C. Anal. calcd (%) for $C_{68}H_{84}Ge_2O_6Zn_2$: C, 64.14; H, 6.65, found: C, 64.37; H, 6.64. ^1H NMR data (C_6D_6, TMS, ppm): 6.43 (s, 4H, Mes-*H*), 6.37 (s, 4H, Mes-*H*), 6.20 (s, 4H, Mes-*H*), 2.58 (s, 12H, Mes-CH_3), 2.21 (s, 12H, Mes-CH_3), 1.97 (s, 12H, Mes-CH_3), 1.95 (s, 18H, Mes-CH_3), 1.75 (s, 18H, C-(CH_3)$_3$). IR (neat): ν(C=O) = 1627, 1607.

Synthesis of ***11***. To a solution of 300 mg of **9** (0.58 mmol; 1.00 equiv) in 10 mL of *n*-heptane, 91 mg of di-*tert*-butylmercury (0.29 mmol; 0.50 equiv) was added. The reaction mixture was brought to 70 °C and stirred overnight. The next day, the reaction mixture was brought to room temperature. The crude product was recrystallized from the reaction solution at −30 °C and filtered off. Yield: 290 mg

https://doi.org/10.1021/acs.organomet.2c00256
Organometallics 2022, 41, 2170−2179

(0.24 mmol; 81%) of analytically pure **11** as a yellow crystalline solid. Mp: 180−182 °C. Anal. calcd (%) for $C_{60}H_{66}Ge_2HgO_6$: C, 58.64; H, 5.41, found: C, 58.87; H, 5.43. ^{13}C NMR data (C_6D_6, TMS, ppm): 238.17 (*C*=O), 144.82 (Mes-*C*4), 139.25 (Mes-C1), 132.14 (Mes-*C*2), 129.45 (Mes-C3), 21.14, 19.52 (Aryl-CH_3). ^1H NMR data (C_6D_6, TMS, ppm): 6.53 (s, 12H, Mes-*H*), 2.19 (s, 36H, Mes-CH_3), 2.08 (s, 18H, Mes-CH_3). UV−vis: λ [nm] (ε [L mol^{-1} cm^{-1}]) = 405 (5094), 389 (6685), 340 (9693). IR (neat): ν(C=O) = 1675, 1645, 1638, 1606.

■ ASSOCIATED CONTENT

Supporting Information

The Supporting Information is available free of charge at https://pubs.acs.org/doi/10.1021/acs.organomet.2c00256.

NMR spectra and X-ray crystallographic information (PDF)

Accession Codes

CCDC 2174956−2174959 contain the supplementary crystallographic data for this paper. These data can be obtained free of charge via www.ccdc.cam.ac.uk/data_request/cif, or by emailing data_request@ccdc.cam.ac.uk, or by contacting The Cambridge Crystallographic Data Centre, 12 Union Road, Cambridge CB2 1EZ, UK; fax: +44 1223 336033.

■ AUTHOR INFORMATION

Corresponding Author

Michael Haas − *Institute of Inorganic Chemistry, Graz University of Technology, 8010 Graz, Austria;* orcid.org/0000-0002-9213-940X; Email: michael.haas@tugraz.at

Authors

Manfred Drusgala − *Institute of Inorganic Chemistry, Graz University of Technology, 8010 Graz, Austria*

Matthias Paris − *Institute of Inorganic Chemistry, Graz University of Technology, 8010 Graz, Austria*

Janine Maier − *Institute of Inorganic Chemistry, Graz University of Technology, 8010 Graz, Austria*

Roland C. Fischer − *Institute of Inorganic Chemistry, Graz University of Technology, 8010 Graz, Austria;* orcid.org/0000-0001-9523-5010

Complete contact information is available at: https://pubs.acs.org/10.1021/acs.organomet.2c00256

Author Contributions

M.D. and M.P. were equally responsible for experimental investigations, formal analysis, visualization, data presentation, and writing the original draft (lead). J.M. was responsible for experimental investigations (supportive). R.C.F. collected the X-ray data and solved the crystal structures. M.H. was in charge of methodology and conceptualization, review and editing of the manuscript (lead), project administration, and funding acquisition.

Funding

Open Access is funded by the Austrian Science Fund (FWF).

Notes

The authors declare no competing financial interest.

■ ACKNOWLEDGMENTS

The authors gratefully acknowledge the FWF (Wien, Austria) for financial support (project number P32606-N).

■ REFERENCES

(1) Biltueva, I. S.; Bravo-Zhivotovskii, D. A.; Kalikhman, I. D.; Vitkovskii, V. Y.; Shevchenko, S. G.; Vyazankin, N. S.; Voronkov, M. G. Sila- and germa-enolate anions. The reaction of acylgermanes with triethylgermyllithium. *J. Organomet. Chem.* **1989**, *368*, 163−165.

(2) Guliashvili, T.; El-Sayed, I.; Fischer, A.; Ottosson, H. The first isolable 2-silenolate. *Angew. Chem., Int. Ed.* **2003**, *42*, 1640−1642.

(3) Bravo-Zhivotovskii, D.; Apeloig, Y.; Ovchinnikov, Y.; Igonin, V.; Struchkov, Y. T. A novel route to the trisilacyclobutane moiety. A possible silene-disilene reaction. *J. Organomet. Chem.* **1993**, *446*, 123−129.

(4) Ohshita, J.; Masaoka, Y.; Masaoka, S.; Ishikawa, M.; Tachibana, A.; Yano, T.; Yamabe, T. Silicon-carbon unsaturated compounds. *J. Organomet. Chem.* **1994**, *473*, 15−17.

(5) Ohshita, J.; Masaoka, S.; Masaoka, Y.; Hasebe, H.; Ishikawa, M.; Tachibana, A.; Yano, T.; Yamabe, T. Silicon−Carbon Unsaturated Compounds. 55. Synthesis and Reactions of Lithium Silenolates, Silicon Analogs of Lithium Enolates. *Organometallics* **1996**, *15*, 3136−3146.

(6) Frühwirt, P.; Knoechl, A.; Pillinger, M.; Müller, S. M.; Wasdin, P. T.; Fischer, R. C.; Radebner, J.; Torvisco, A.; Moszner, N.; Kelterer, A.-M.; Griesser, T.; Gescheidt, G.; Haas, M. The Chemistry of Acylgermanes: Triacylgermenolates Represent Valuable Building Blocks for the Synthesis of a Variety of Germanium-Based Photoinitiators. *Inorg. Chem.* **2020**, *59*, 15204−15217.

(7) Püschmann, S. D.; Frühwirt, P.; Pillinger, M.; Knöchl, A.; Mikusch, M.; Radebner, J.; Torvisco, A.; Fischer, R. C.; Moszner, N.; Gescheidt, G.; Haas, M. Synthesis of Mixed-Functionalized Tetraacylgermanes. *Chem. - Eur. J.* **2021**, *27*, 3338−3347.

(8) Drusgala, M.; Linden, M. H.; Knoechl, A.; Torvisco, A.; Fischer, R. C.; Bernhard Linden, H.; Haas, M. Synthesis, LIFDI Mass Spectrometry and Reactivity of Triacyl-Germenolates. *Eur. J. Inorg. Chem.* **2021**, *2021*, 3091−3096.

(9) Haas, M. Recent Advances in the Chemistry of Heavier Group 14 Enolates. *Chem. - Eur. J.* **2019**, *25*, 15218−15227.

(10) Ohshita, J.; Masaoka, S.; Ishikawa, M. Oxidative Coupling of Lithium Silenolates: First Synthesis of Bis(acyl)-Substituted Polysilanes. *Organometallics* **1996**, *15*, 2198−2200.

(11) Haas, M.; Fischer, R.; Flock, M.; Mueller, S.; Rausch, M.; Saf, R.; Torvisco, A.; Stueger, H. Stable Silenolates and Brook-Type Silenes with Exocyclic Structures. *Organometallics* **2014**, *33*, 5956−5959.

(12) Haas, M.; Leypold, M.; Schnalzer, D.; Torvisco, A.; Stueger, H. Stable Germenolates and Germenes with Exocyclic Structures. *Organometallics* **2015**, *34*, 5291−5297.

(13) Haas, M.; Leypold, M.; Schnalzer, D.; Torvisco, A.; Stueger, H. Synthesis and characterization of the first relatively stable dianionic germenolates. *Phosphorus Sulfur Silicon Relat. Elem.* **2016**, *191*, 597−600.

(14) Haas, M.; Leypold, M.; Schuh, L.; Fischer, R.; Torvisco, A.; Stueger, H. Reactivity of Cyclic Silenolates Revisited. *Organometallics* **2017**, *36*, 3765−3773.

(15) Drusgala, M.; Frühwirt, P.; Glotz, G.; Hogrefe, K.; Torvisco, A.; Fischer, R.; Wilkening, H. M. R.; Kelterer, A.-M.; Gescheidt, G.; Haas, M. Isolable Geminal Bisgermenolates: A New Synthon in Organometallic Chemistry. *Angew. Chem., Int. Ed.* **2021**, *60*, 23646−23650.

(16) Maier, J.; Müller, S. M.; Torvisco, A.; Glotz, G.; Fischer, R. C.; Griesser, T.; Kelterer, A.-M.; Haas, M. Isolable Stannenolates Enable the Synthesis of Visible-Light Photoinitiators. *ChemPhotoChem* **2021**, *6*, No. e202100213.

(17) Teng, W.; Ruhlandt-Senge, K. Syntheses and structures of the first heavy-alkali-metal tris(trimethylsilyl)germanides. *Chem. - Eur. J.* **2005**, *11*, 2462−2470.

(18) Marschner, C. A New and Easy Route to Polysilanylpotassium Compounds. *Eur. J. Inorg. Chem.* **1998**, 221−226.

(19) North, M. Edited By Jacob Zabicky The Chemistry of Metal Enolates-Part 1 Wiley, 2009, 577 pp. (part 1; 1250 pp., parts 1 and 2) (parts 1 and 2; hardback) ISBN 978-0-470-06168-8. *Appl. Organometal. Chem.* **2010**, 426−427.

(20) Grison, C.; Petek, S.; Coutrot, P. Preparation of Magnesium Enolates of α-Keto Esters and Synthetic Applications. *Synlett* **2005**, *2*, 331−333.
(21) Nanjo, M.; Oda, T.; Sato, T.; Mochida, K. Synthesis and oxidation of bis(triphenylgermyl)zinc. *J. Organomet. Chem.* **2005**, *690*, 2952−2955.
(22) Nanjo, M.; Oda, T.; Mochida, K. Preparation and structural characterization of trimethylsilyl-substituted germylzinc halides, $(Me_3Si)_3GeZnX$ (X = Cl, Br, and I) and silylzinc chloride, $R(Me_3Si)_2SiZnCl$ (R=$SiMe_3$ and Ph). *J. Organomet. Chem.* **2003**, *672*, 100−108.
(23) Nanjo, M.; Oda, T.; Mochida, K. Preparation and Characterization of Tris(trimethylsilyl)germylzinc Chloride and Bis[tris(trimethylsilyl)germyl]zinc. *Chem. Lett.* **2002**, *31*, 108−109.
(24) Castel, A.; Rivière, P.; Satgé, J.; Ko, Y. H.; Desor, D. Trimésitylgermyllithium: Synthèse et réactivité. *J. Organomet. Chem.* **1990**, *397*, 7−15.
(25) Brook, A. G.; Abdesaken, F.; Söllradl, H. Synthesis of some tris(trimethylsilyl)germyl compounds. *J. Organomet. Chem.* **1986**, *299*, 9−13.
(26) Fischer, J.; Baumgartner, J.; Marschner, C. Silylgermylpotassium Compounds. *Organometallics* **2005**, *24*, 1263−1268.
(27) Dobrovetsky, R.; Kratish, Y.; Tumanskii, B.; Botoshansky, M.; Bravo-Zhivotovskii, D.; Apeloig, Y. Radical activation of Si-H bonds by organozinc and silylzinc reagents: synthesis of geminal dizinciosilanes and zinciolithiosilanes. *Angew. Chem., Int. Ed.* **2012**, *51*, 4671−4675.
(28) Radebner, J.; Leypold, M.; Eibel, A.; Maier, J.; Schuh, L.; Torvisco, A.; Fischer, R.; Moszner, N.; Gescheidt, G.; Stueger, H.; Haas, M. Synthesis, Spectroscopic Behavior, and Photoinduced Reactivity of Tetraacylgermanes. *Organometallics* **2017**, *36*, 3624−3632.
(29) Haas, M.; Radebner, J.; Eibel, A.; Gescheidt, G.; Stueger, H. Recent Advances in Germanium-Based Photoinitiator Chemistry. *Chem. - Eur. J.* **2018**, *24*, 8258−8267.
(30) Pangborn, A. B.; Giardello, M. A.; Grubbs, R. H.; Rosen, R. K.; Timmers, F. J. Safe and Convenient Procedure for Solvent Purification. *Organometallics* **1996**, *15*, 1518−1520.
(31) Chisholm, M. H.; Drake, S. R.; Naiini, A. A.; Streib, W. E. Synthesis and X-ray crystal structures of the one-dimensional ribbon chains [MOBut·ButOH]∞ and the cubane species $[MOBut]_4$ (M = K and Rb). *Polyhedron* **1991**, *10*, 337−345.
(32) Blaukat, U.; Neumann, W. P. Synthesen mit Verbindungen R_3M-Hg-MR_3 und $(R_2M\text{-}Hg)_n$ (M = C, Si, Ge, Sn): XI. Mercurierung und Demercurierung mittels di-*t*-butylquecksilber, $(CH_3)_3C\text{-}Hg\text{-}C(CH_3)_3$. *J. Organomet. Chem.* **1973**, *49*, 323−332.
(33) Kondo, Y.; Shilai, M.; Uchiyama, M.; Sakamoto, T. TMP−Zincate as Highly Chemoselective Base for Directed Ortho Metalation. *J. Am. Chem. Soc.* **1999**, *121*, 3539−3540.
(34) Radebner, J.; Eibel, A.; Leypold, M.; Gorsche, C.; Schuh, L.; Fischer, R.; Torvisco, A.; Neshchadin, D.; Geier, R.; Moszner, N.; Liska, R.; Gescheidt, G.; Haas, M.; Stueger, H. Tetraacylgermanes: Highly Efficient Photoinitiators for Visible-Light-Induced Free-Radical Polymerization. *Angew. Chem., Int. Ed.* **2017**, *56*, 3103−3107.
(35) Bruker *APEX2 and SAINT*; Bruker AXS Inc.: Madison, Wisconsin, USA, 2012.
(36) Blessing, R. H. An empirical correction for absorption anisotropy. *Acta Crystallogr., Sect. A: Found. Crystallogr.* **1995**, *51*, 33−38.
(37) Sheldrick, G. M. Phase annealing in SHELX-90: direct methods for larger structures. *Acta Crystallogr., Sect. A: Found. Crystallogr.* **1990**, *46*, 467−473.
(38) Sheldrick, G. M. A short history of SHELX. *Acta Crystallogr., Sect. A: Found. Crystallogr.* **2008**, *64*, 112−122.
(39) Sheldrick, G. M. SHELXT - integrated space-group and crystal-structure determination. *Acta Crystallogr., Sect. A: Found. Adv.* **2015**, *71*, 3−8.
(40) Dolomanov, O. V.; Bourhis, L. J.; Gildea, R. J.; Howard, J.A.K.; Puschmann, H. OLEX2: a complete structure solution, refinement and analysis program. *J. Appl. Crystallogr.* **2009**, *42*, 339−341.
(41) Spek, A. L. Single-crystal structure validation with the program PLATON. *J. Appl. Crystallogr.* **2003**, *36*, 7−13.
(42) Spek, A. L. Structure validation in chemical crystallography. *Acta Crystallogr., Sect. D: Biol. Crystallogr.* **2009**, *65*, 148−155.
(43) Müller, P.; Herbst-Irmer, R.; Spek, A.; Schneider, T.; Sawaya, M. *Crystal Structure Refinement: A Crystallographer's Guide to SHELXL*; Oxford University Press, 2006.

https://doi.org/10.1021/acs.organomet.2c00256
Organometallics 2022, 41, 2170−2179